LIGHT SOURCE

& BEAMLINES

Measurement of the Bunch Length of the UVSOR Storage Ring

Akihiko LIN*, Hiroyuki HAMA, Shirou TAKANO and Goro ISOYAMA

* Institute for Solid State Physics, University of Tokyo, Roppongi, Minatoku, Tokyo 106
Institute for Molecular Science, 38 Myodaiji, Okazaki 444

The bunch length of the UVSOR storage ring has been measured with the single photon counting method over wide ranges of beam energies from 500 to 750 MeV and stored beam currents from 100 μA to about 60 mA in the single bunch operation mode. The synchrotron radiation emitted in one of the bending magnets is detected with a fast photomultiplier. A time difference between signals from the photomultiplier and the revolution frequency is analyzed with a conventional time analyzing system. The overall time resolution of the detection system is estimated to be 194 pses (FWHM). The synchrotron frequency was also measured when a beam current is less than 1 mA.

The following three kinds of measurements have been made;

(a) dependence of the bunch length and the synchrotron frequency at E=750 MeV on the RF accelerating voltage. The beam current is kept less than 1 mA in order to avoid influences of the collective effect.

(b) dependence of the bunch length and the synchrotron frequency on the beam energy. The beam current is kept less than 1 mA and the RF voltage is fixed at a nominal value, about 50 kV.

(c) dependence of the bunch length on the beam current in the energy region from 500 to 750 MeV. The RF voltage is kept at the nominal value.

In the analysis, it is assumed that an energy spread of the electron beam is given by the single particle theory, an equilibrium distribution determined by quantum excitation and radiation damping, and the energy of an electron is lost only by emission of the synchrotron radiation, when the beam current is low at E=750 MeV. From the experimental result in the measurement (a) and the above assumptions, the time resolution of the measurement system and the momentum compaction factor α are estimated, and the RF voltage is calibrated. From the measurements (a) and (b), it is confirmed that the electron energy and the RF voltage dependences of the bunch length agree well with the predictions of the single particle theory.

Figure 1 shows the current dependent bunch lengthening of the UVSOR storage ring at various beam energies. The bunch length becomes longer when the beam current is larger than a few mA, and the bunch lengthening is larger when the beam energy is lower. This behavior does not agree with a prediction of the microwave instability[1)] that the bunch length becomes long as the 1/3 power of the beam current. The experimental bunch lengthening of the UVSOR storage ring shown in Fig. 1 is well reproduced by the potential distortion theory[2)] if the effective impedance is taken as a free parameter. The effective impedances estimated above are shown in Fig. 2 as a function of bunch length. Although they are estimated from data taken at various beam currents and energies, all the points in Fig. 2 are located around a single curve, which varies smoothly from about 1.2 to 0.2 Ω as the bunch length changes from 0.033 to 0.055 m. This fact assures us that the bunch lengthening of the UVSOR storage ring is dominated by the potential distortion.

References

1) A.W. Chao, AIP Conf. Proc. **105**, 1982, p.353.
2) J.L. Laclare, Cern **87-03**, 1987, p.264.

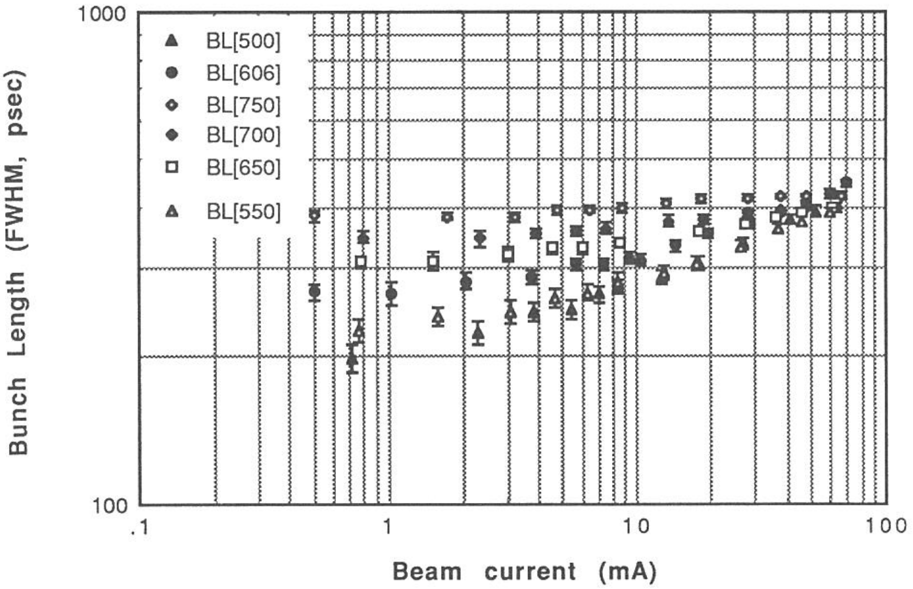

Fig.1. Bunch Lengthening of the UVSOR Storage Ring

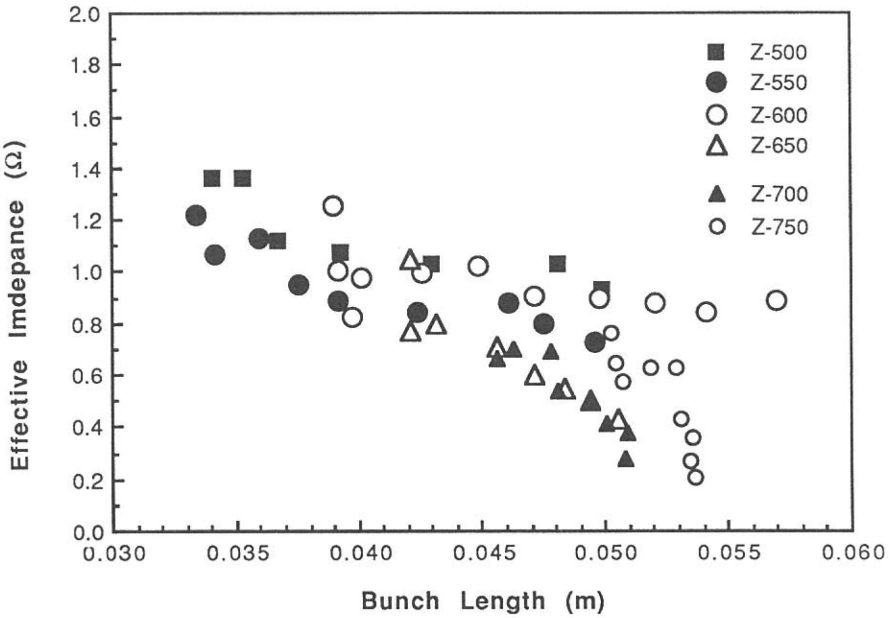

Fig. 2. Effective impedance as a function of bunch length

Free Electron Laser Experiment on the UVSOR Storage Ring

Shirou TAKANO, Hiroyuki HAMA, Goro ISOYAMA, and Akihiko LIN*

Institute for Molecular Science, 38 Myodaiji, Okazaki 444
*Institute for Solid State Physics, The University of Tokyo, Roppongi, Minatoku, Tokyo 106

A free electron laser (FEL) experiment is now being carried out on the UVSOR storage ring. The wavelength of light has been chosen to be 488 nm for an electron energy of 500 MeV.

For a gain measurement experiment, a conventional transverse undulator made of permanent magnets is employed for the moment, and is installed in one of the long straight sections of the storage ring. The period length and the number of periods of the undulator are 111 mm and 19, respectively. Electrons are stored in one of the 16 RF buckets (the single bunch operation) by the full energy injection. So far, the maximum stored beam current (average) I is about 60 mA. The beam life time is 25 min. at I = 50 mA, and is 70 min. at I = 10 mA. The peak current, which is estimated from a measurement of the longitudinal bunch length[1), is 5 A for the beam current I = 10 mA, whereas it is 19 A for I = 50 mA due to the bunch lengthening. The horizontal and the vertical beam sizes at the center of the straight section are $\sigma_h = 0.7$ mm and $\sigma_v = 0.1$ mm, respectively. The theoretical small-signal gain per pass estimated for the above conditions is $3\times10^{-3}(I/10\mathrm{mA})\mathcal{F}$, where $\mathcal{F}$ is a filling factor calculated from an overlap between the laser beam and the electron beam. Figure 1 shows an experimental arrangement for the gain measurement. An argon ion laser of 1 W (CW) output power is used as the external light, which is injected through a glass window into the straight section. The laser beam is focused to a waist near the center of the undulator by a mode matching telescope, and a direction of is varied with a frequency of about 100 kHz by a photoelastic modulator. The output light from the exit glass window passes through two irises and a bandpass filter, which reduce unwanted spontaneous emission from the undulator, and is focused to a fast photodiode. The signal from the detector is amplified and processed by an spectrum analyzer. The signal due to stimulated emission or absorption is doubly modulated by the revolution frequency of the electron bunch (f_{rev} = 5.6 MHz) and by the modulation frequency of the laser beam (f_{mod} ~ 100 kHz), and it is observed as the side bands of the revolution frequency at $f_{rev} \pm f_{mod}$. A preliminary result of the experiment is given in figure 2. The upper panel shows the intensity of spontaneous emission as a function of the undulator gap. The lower panel shows the intensity of the sideband (open circles), which is proportional to an amplitude of the gain or loss, as well as a fit using an theoretical gain curve calculated from the spontaneous emission spectrum shown above (Maday's theorem). The measured peak gain without correction of the filling factor is estimated to be roughly 10^{-3} for the stored beam current I of 10 mA. We are now trying to obtain an accurate calibration of the peak gain.

For the next step, we plan to employ an undulator with the optical klystron configuration in order to increase the gain. The central three periods of the present undulator will be transformed into the dispersive section of the optical klystron by re-arranging magnet blocks. The magnet gap of the dispersive section can be varied independently of the normal undulator sections. We have chosen an optimum value of N_d to be 72, which is the number of light waves passing over an electron in the dispersive section. The estimated gain becomes 6-8 times higher than that with the conventional undulator for the energy spread of the electron beam σ_E/E = (5-10)$\times 10^{-4}$. After an amplifier experiment with this optical klystron, we will proceed to an oscillator experiment.

Acknowledgement: We are grateful to Dr. N. A. Vinokurov for his technical and theoretical suggestions for the experiment.

References

1) A. Lin 1991, Master Thesis, The University of Tokyo; A. Lin, H. Hama, S. Takano and G. Isoyama, a report in this volume.

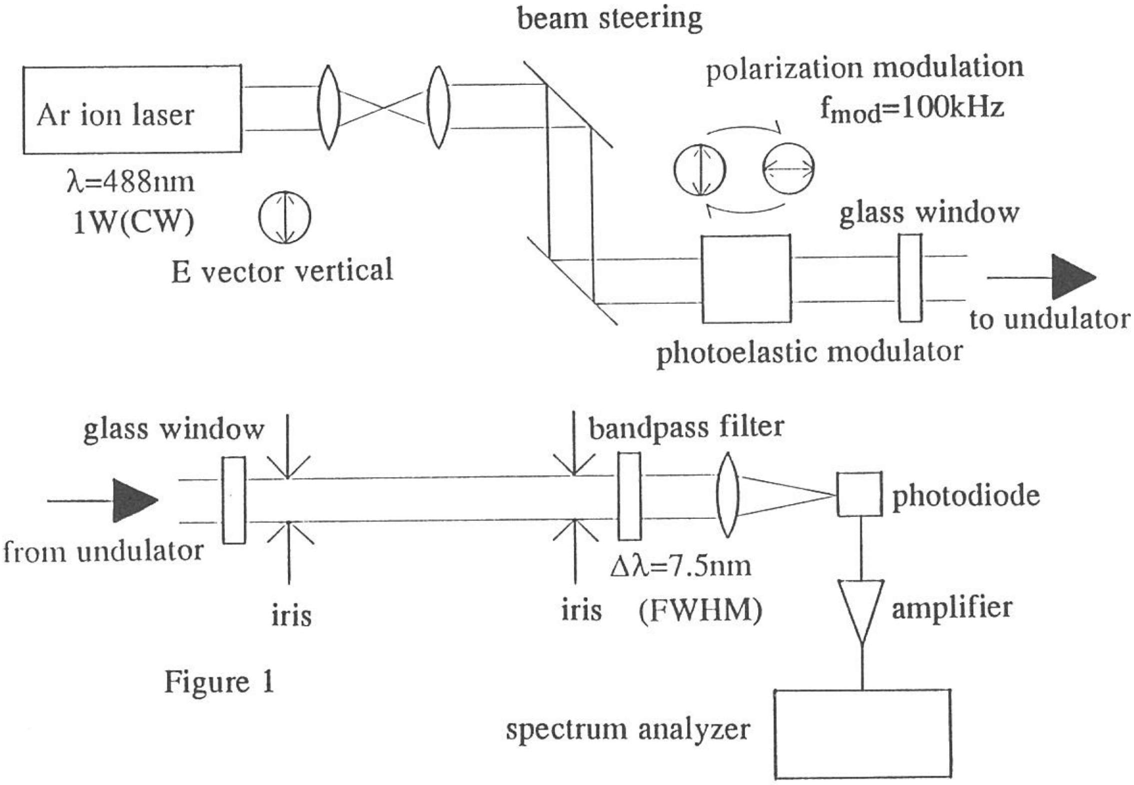

Figure 1

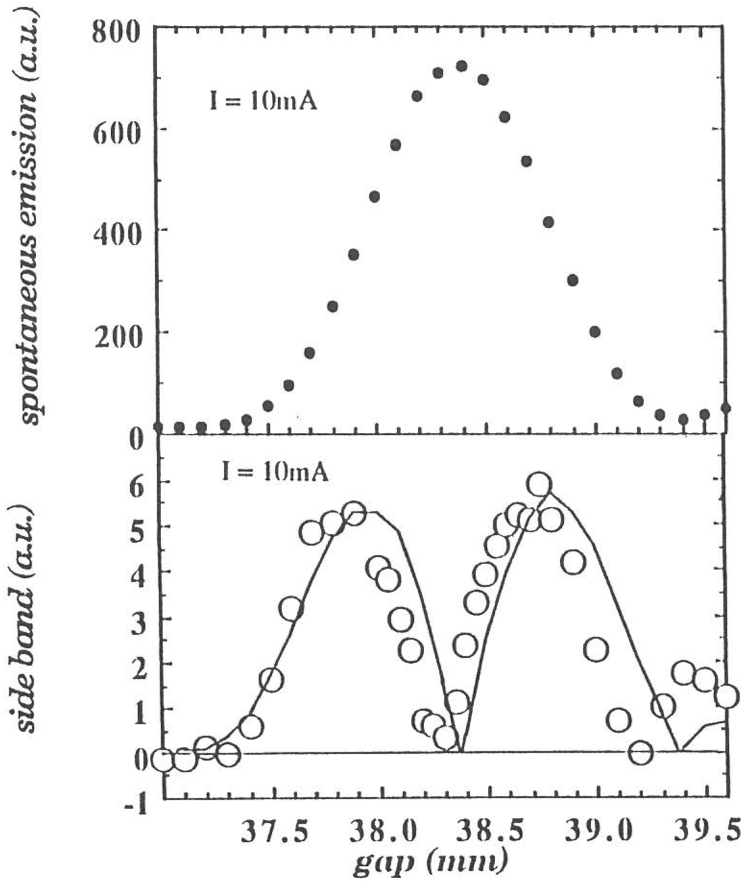

Figure 2

Construction of Beam Lines

M. Kamada and M. Watanabe

Institute for Molecular Science, Myodaiji, Okazaki 444

We are constructing four beam lines (BL1A, BL4A, BL4B, and BL6B). BL1A is designed for soft x-ray spectroscopy on gas and solids. Beam line valves, a pre-mirror chamber, and a double-crystal monochromator chamber have been constructed last autumn. The test of monochromator will be carried out this winter. BL4A and BL4B serve for photolysis and photo-chemical reaction experiments on solid surfaces. These beam lines consist of valves, pre-mirror chambers, reaction chambers, and analysing instruments. Both focused and unfocused synchrotron radiation can be supplied. BL6B is used for infrared spectroscopy. Beam line valves, a pre-mirror chamber, and a window chamber have been constructed last autumn. An interferometer equipped with a microscope will be installed this winter. Synchrotron radiation through various ir-window materials can be used at this beam line.

Thus, we have now nineteen beam lines at UVSOR Facility (see Table II in Appendix). Nine of them (BL1A, BL2A, BL2B2, BL3B, BL4A, BL4B, BL6A2, BL6B, and BL8B2) are mainly used by in-house staffs of IMS (outside researchers can also use them), one of them (BL5B) is belonging to National Institute for Fusion Science, and the others (BL1B, BL2B1, BL3A1, BL3A2, BL6A1, BL7A, BL7B, BL8A, and BL8B1) are opened to both inside and outside users of IMS. There are four 1m Seya-Namioka, one 3m normal incidence, three plane grating, three grazing incidence and two double-crystal motochromators for vacuum ultraviolet and soft x-ray, and one interferometer for far infrared. An interferometer for infrared will be installed soon at BL6B.

Construction of New Soft X-ray Beam Line at BL1A

Atsunari HIRAYA, Toshio HORIGOME, Norio OKADA, Nobuo MIZUTANI, Kusuo SAKAI, Osamu MATSUDO, Masami HASUMOTO, Kazutoshi FUKUI[†] and Makoto WATANABE

Institute for Molecular Science, Myodaiji, Okazaki 444
[†]Department of Electrical and Electronics Engineering, Fukui University, Fukui 910

A new soft X-ray beam line equipped with a double crystal monochromator (DXM) has been constructed at BL1A. In order to gather synchrotron radiation and focus it at the sample position a pre-mirror is used for this beam line, which is the main difference between BL1A and the existing soft X-ray beam line BL7A. Both the minimum reflection loss in the soft X-ray region and the good focusing without astigmatism at the sample position are required for this mirror. In order to fulfill these requirements the grazing angle of 1 ° was selected and a cylindrical mirror (550 mm long, 30 mm wide, 15 mm thick, 50.5 mm curvature, Pt coated) was elliptically bent for horizontal focusing by pressing on an elliptic surface of the mirror holder. With this pre-mirror horizontal acceptance angle of BL1A is 4.2 mrad which is about two times wider than that of BL7A. Focused spot size of the monochromatized X-ray measured by a multi-channel-plate with phosphor screen was 2 mm wide and 1 mm high at the sample position.

Figure 1 shows the scanning mechanism of the new DXM which is essentially the same with the DXM at BL7A.[1] Fixed direction and constant offset of the monochromatized X-ray beam during the change of Bragg angle is realized as follows. By linear-guides indicated by horizontal arrows, vertical positions of the centers of the first and second crystal surfaces are confined on the levels of the incident and

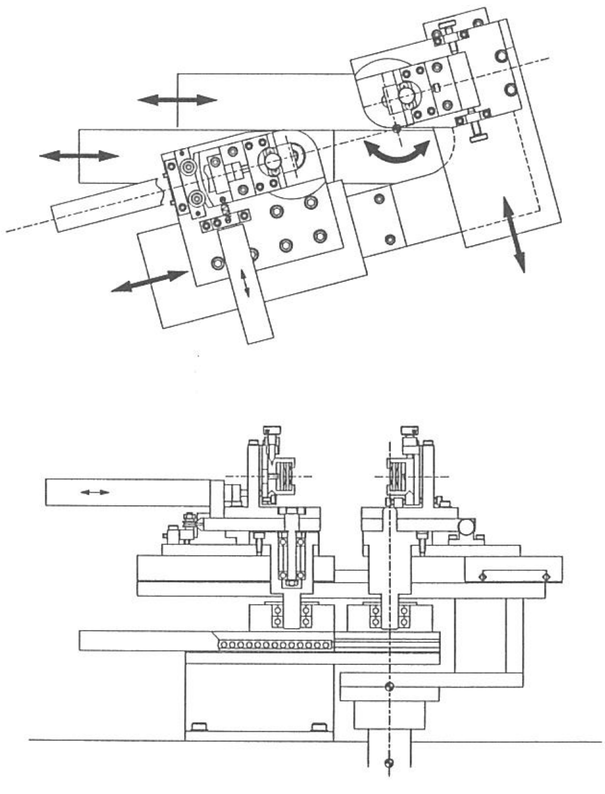

Figure 1. Drawing of the scanning mechanism of the double crystal monochromator at BL1A.

monochromatized beams, respectively. By other linear-guides indicated by slanting arrows moving along each arm of a L-shaped base, the crystal surfaces are kept parallel with each other. Scanning of Bragg angle is introduced by the rotation of the L-shaped base indicated by a curved arrow. For each crystal a pair of the former and the latter linear-guides are linked at the rotation axis on the crystal surface. Therefore the angles and horizontal positions of two crystals are synchronously driven so that the first and second crystals reflect the beam at their center of crystal surface at any Bragg angle to the fixed direction with constant offset. In order to angle adjustments of the second crystal with keeping vacuum of the monochromator chamber, two motorized-screws with encoders (Oriel Encoder Mike™) are used.

Figure 2 shows the throughput spectrum of BL1A behind the double crystal monochromator with beryl crystals measured by an electron multiplier tube (EMT) with an Au first dynode. Compared with the throughput spectrum of BL7A (DXM with another pair of beryl crystals) measured by the same EMT, the throughput of BL1A is found to be 3 ~ 4 times higher than that of BL7A over the scanning range of the DXM.

1) T.Murata, T.Matsukawa, M.Mori, M.Obashi, S.Naoe, H.Terauchi, Y.Nishihata, O.Matsudo and J.Yamazaki. J. de Phys. **C8** (1986) 135.

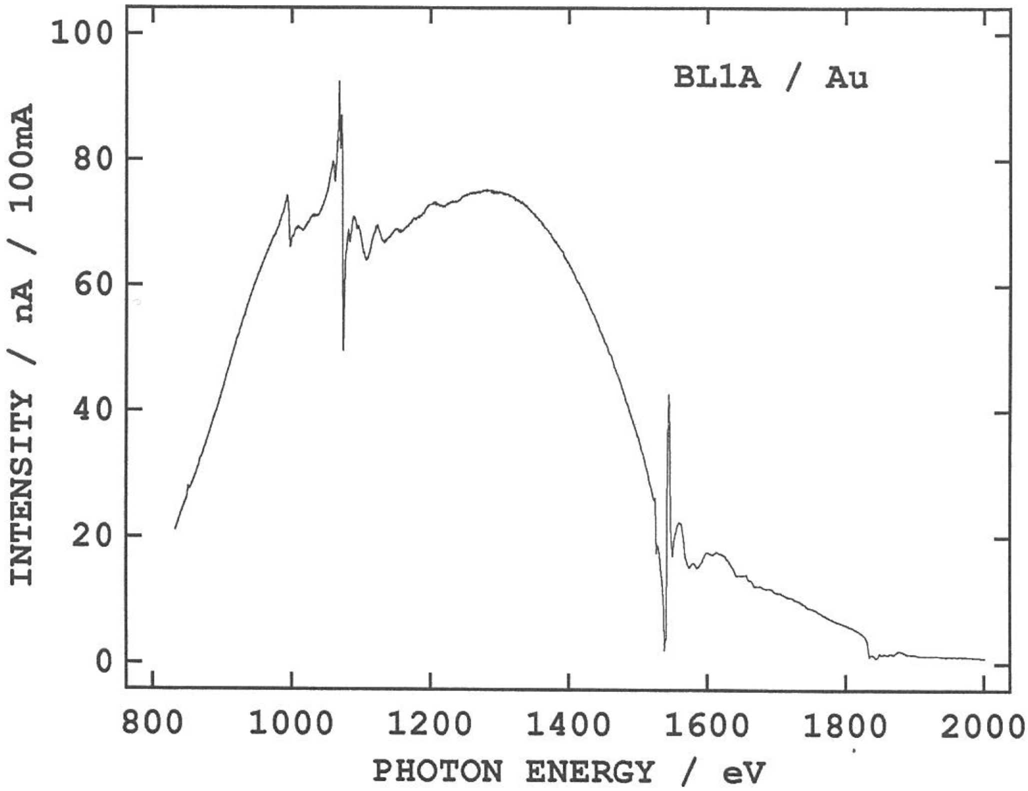

Figure 2. Throughput spectrum of double crystal (Beryl) monochromator at BL1A.

Utilization of Multilayers as the Dispersive Element of Soft X-Ray Monochromator

M. Watanabe, O. Matsudo, J. Yamazaki, S. Takahama* and K. Yamashita**

UVSOR, Institute for Molecular Science
*Department of Physics, Faculty of Science, Osaka University
**Institute for Space and Astronautical Science

Recently, multilayers have been developed extensively in the VUV and soft X-ray region as the efficient reflectors.[1)] Since the reflectivity is enhanced at the wavelength which satisfies the usual Bragg condition $n\lambda=2d\sin\theta$, the multilayers can be used as a dispersive element. The resolution is the order of 10^{-2}.

For a double crystal monochromator (DXM) at BL7A,[2)] a pair of beryl crystals is used as the dispersive element below 15 Å. Above 15 Å a KAP crystal is a candidate of the dispersive element. However, it is weak against the strong irradiation of synchrotron radiation, so that it can not be used as the first crystal of the DXM. In this experiment, instead of the KAP crystal a multilayer (W/Si) with 2d=53.2 Å is used as the first dispersive element and the KAP crystal (2d=26.6 Å) was used as the second dispersive element. In this case, the second order light (n=2) dispersed with the multilayer is again dispersed by the KAP crystal in the first order. Figure 1 a) shows the output photon flux distribution detected by a nude photomultiplier with a photocathode coated with Nacl. One can see O-K absorption of BeO which is the substrate material of the photocathode around 550 eV and Na-K absorption of NaCl around 1070 eV. The intensity decreases with the decrease in the photon energy below Na-K edge. This feature may be due to the reflection characteristics of the multilayer in the second order and the absorption of a Be foil of 5 μm thickness, which is located in front of the DXM to separate the vacuum of the DXM from that of the front end of BL7A. Figure 1 b) shows the detailed spectra around Na-K edge. The curve 1 is the spectrum obtained without the collimation of the beam. The resolution is low. The curve 2 shows the spectrum obtained with the collimation of the incident and dispersed beams with two pinholes of which diameters are 0.8 mm. The resolution is improved, but not so good as that by using a pair of beryl crystals (curve 3).

Another experiment is now under way to get higher photon flux with less resolution by the use of a pair of multilayers (W/B_4C) with 2d=31.2 Å in the first order.

References

1) Proc. Int. Conf. Soft X-ray Optics and Technology, Berlin 1986, Proc. SPIE **733** (1987), p.307.
2) T. Murata et al.: J. de Phys. **C8** (1986) 135.

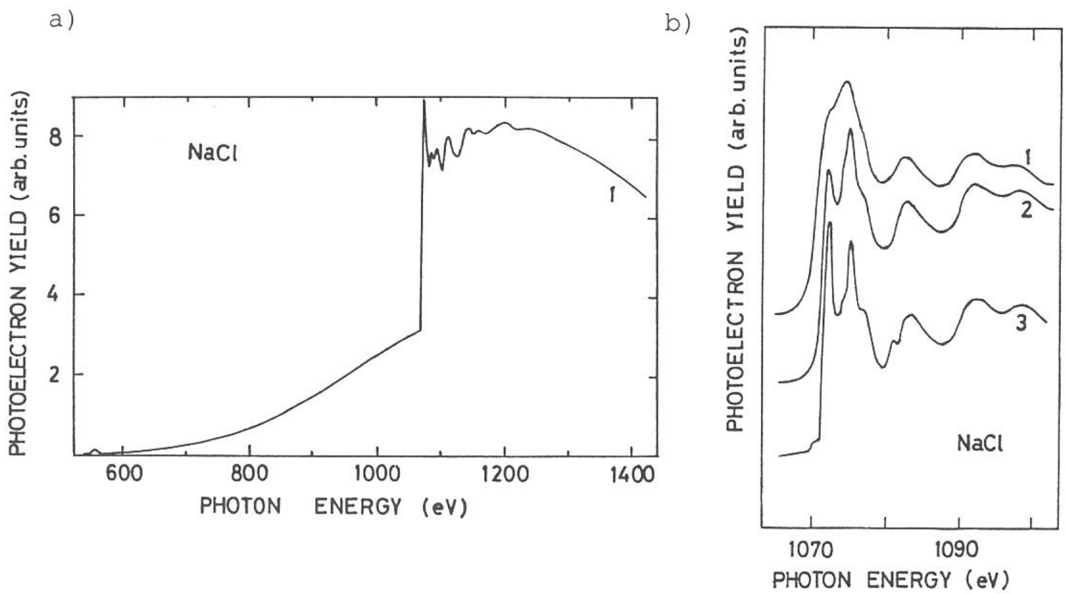

Fig.1. Output spectra from DXM detected by a nude photomultiplier with a NaCl coated photocathode, a) in the 550-1400 eV and b) 1070-1100 eV region. Curves 1 and 2 are spectra obtained by using a multilayer (W/Si, 2d=53.2 Å) as the first disperse element and a KAP crystal as the second one, without and with collimator of two pinholes with 0.8 mm diameter, respectively and curve 3, spectrum obtained by using a pair of beryl crystals.

Construction of the Second Experimental Chamber and Interchanging Mechanism for Focusing Mirrors

Makoto SAKURAI and Eiji ISHIGURO *

National Institute for Fusion Science, Nagoya 464-01
*Faculty of Engineering, Osaka City University, Osaka 558

BL5B is dedicated for various radiometric research projects in the wavelength range from VUV to SX. The experimental chamber of the beam line enables calibration and characterization of various type of optical elements and detectors [1], however, ultimate pressure of the chamber ($1x10^{-8}$ Torr) is insufficient for basic research such as to identify physical processes in surface sensitive detectors and clarify the correlation between surface structures and optical characteristics.

Under this necessity, the second experimental chamber was constructed and installed on the beam line at 3.3m downstream from the focusing mirror (M_3) of the plane grating monochromator (PGM) [2] as shown in Fig. 1. Since the original mirror has a focal point at 1.1m position (Q_1), we needed the second toroidal mirror for the other focal point (Q_2). Then, we calculated optimum parameters and manufactured a new mirror and a mirror holder which accomodates two focusing mirrors and enables to interchange the mirrors in vacuum. Fig. 2 shows calculated beam size at Q_2 for each combination of gratings and mirrors of the PGM with the optimized parameters; the radii of the toroid are R_V=23278mm and R_H=67mm for vertical and horizontal directions, respectively. Fig. 3 shows cross sectional view of the interchanging mechanism. The mirrors have three degrees of freedom: tilting around two axes and translation along horizontal direction perpendicular to the optical axis. Observed beam size was 2x5 mm^2 for the visible part of the 0th order light. The second experimental chamber, 450mmϕx700mm in size, is evacuated by a turbo-molecular pump, a sputter ion pump and a titanium sublimation pump with liquid nitrogen shroud, and is equipped with two (co-axial) rotational stages at the bottom of the chamber. Between the two experimental chambers, a rare gas ionization chamber is inserted to measure the absolute intensity of incident photon flux in the VUV regions. Positions of both entrance and exit windows of the chamber are adjustable in vacuum. This part also works as a differential pumping stage which enables an experiment with SR light in the 10^{-10} Torr range at the second chamber while the first chamber remaining in the 10^{-8} Torr range.

References

1) M. Sakurai et al., Vacuum **41**, 1234 (1990).

2) M. Sakurai et al., Rev. Sci. Instrum. **60**, 2089 (1989).

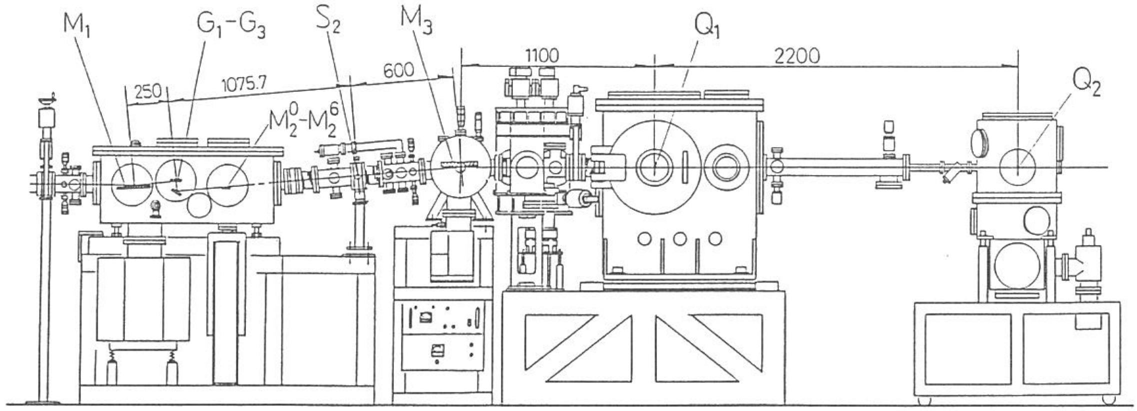

Fig. 1. Schematic diagram of BL5B.

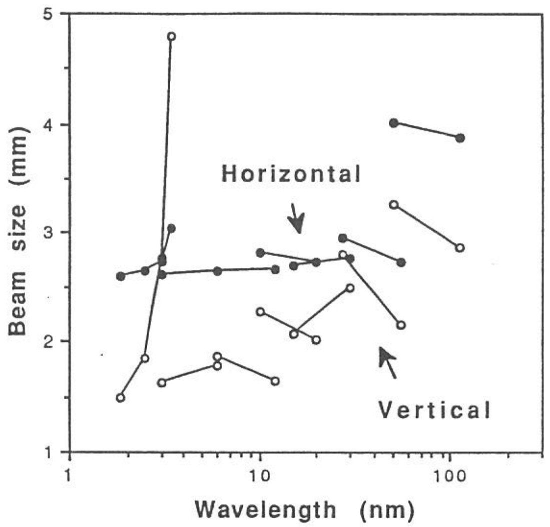

Fig. 2. Calculated beam size at Q_2.

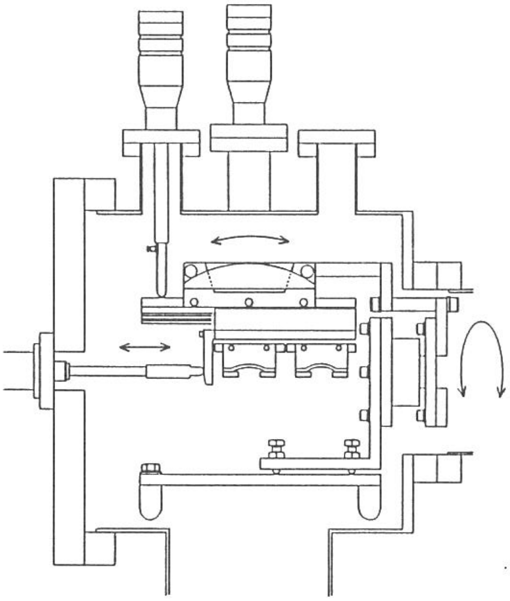

Fig. 3. Cross sectional view of interchanging mechanism for focusing mirrors.